Optical excitation of phase modes in strongly disordered superconductors

T. Cea,[1] D. Bucheli,[1] G. Seibold,[2] L. Benfatto,[1] J. Lorenzana,[1] and C. Castellani[1]
[1]*ISC-CNR and Department of Physics, "Sapienza" University of Rome, Piazzale A. Moro 5, 00185 Rome, Italy*
[2]*Institut Für Physik, BTU Cottbus, P.O. Box 101344, 03013 Cottbus-Senftenberg, Germany*
(Received 20 December 2013; revised manuscript received 17 April 2014; published 12 May 2014)

According to the Goldstone theorem the breaking of a continuous U(1) symmetry comes along with the existence of low-energy collective modes. In the context of superconductivity these excitations are related to the phase of the superconducting (SC) order parameter and for clean systems are optically inactive; that is, single-mode excitations do not directly couple to light. Here we show that for strongly disordered superconductors phase modes acquire a dipole moment and appear as a subgap spectral feature in the optical conductivity. This finding is obtained with both a gauge-invariant random-phase approximation scheme based on a fermionic Bogoliubov–de Gennes state and a prototypical bosonic model for disordered superconductors. In the strongly disordered regime, where the system displays an effective granularity of the SC properties, the optically active dipoles are linked to the isolated SC islands, offering a new perspective for realizing microwave optical devices.

DOI: 10.1103/PhysRevB.89.174506 PACS number(s): 74.20.−z, 74.25.Gz, 74.62.En

I. INTRODUCTION

In the last decades the failure of the BCS paradigm of superconductivity in several materials led to a profound modification of the description of the superconducting (SC) phenomenon itself. A case in point is the occurrence of Cooper pairing and phase coherence at distinct temperatures, associated with the appearance of a single-particle gap Δ and a nonzero superfluid stiffness D_s, respectively. This behavior is observed, e.g., in high-temperature cuprate superconductors [1,2], in strongly disordered films of conventional superconductors [3–8], and, recently, also in SC heterostructures [9]. In all these materials the BCS prediction that D_s is of order of the Fermi energy, much larger than $\Delta \sim T_c$, is violated due to the strong suppression of D_s. The resulting scenario, supported by systematic tunneling measurements, suggests that pairing survives above T_c, leading to a pseudogap state dominated by phase fluctuations enhanced by the low D_s value [10].

In all this, optics represents a preferential playground to address the peculiar role of disorder. Indeed, as we shall see, disorder renders collective modes, which are optically inactive in a clean superconductor, visible. The possibility that in the presence of quenched disorder phase fluctuations can induce a finite-frequency absorption has been discussed in the past within the context of high-temperature cuprates [11,12], where an excess optical absorption has been measured in the microwave regime [11], and, more recently, within the context of conventional disordered superconductors [13]. However, due to the complexity of these materials, the previous literature focused mostly on phenomenological models for the phase degrees of freedom, leaving open their relevance for a more realistic description of conventional superconductors, where deviations from dirty BCS theory have recently been reported as well [14–17]. While more recent attempts have been made to describe the superconductor-insulator transition (SIT) within minimal bosonic models for disorder, like the diluted quantum XY model [13], it has not been established yet if in conventional superconductors with a small SC gap the collective-mode absorption occurs below the threshold for a photon to break apart a Cooper pair. It has been recently suggested, by extending previous work in the same context [18,19], that within Lorentz-invariant models the amplitude fluctuations of the SC order parameter can give rise to subgap absorption even in the clean case when the quantum-critical point for SC destruction is approached [20]. However, these processes involve excitations of multiple (amplitude and phase) bosonic modes, so that they are expected to be subleading with respect to direct one-mode phase excitations, which is the issue discussed in the present work. In addition, the behavior of amplitude fluctuations in the presence of disorder in a system far from criticality, where the dynamics of amplitude fluctuations is known not to be Lorentz invariant [21–23], is another question still open. Finally, in the last few years the systematic investigation of strongly disordered conventional superconductors by means of real-space probes like scanning tunnel microscopy (STM) [5,8] revealed an emergent granularity of the SC properties induced by even homogeneous disorder. It would be interesting, as suggested in a recent experiment performed above T_c [24], to establish a connection between this real-space image and the low-temperature response of the system excited at a finite frequency.

In this paper we address all the above issues by computing the optical conductivity within two prototypical fermionic and bosonic models for disordered superconductors. First, we consider as a microscopic *fermionic* model the attractive Hubbard model with on-site disorder, which has already been shown to reproduce several features observed in strongly disordered conventional superconductors [25–30]. We show that thanks to the breaking of translational invariance the collective modes couple to light via an intermediate particle-hole excitation process. Most remarkable, this coupling leads to the emergence of additional optical absorption, mainly due to phase modes, *below* the BCS-like threshold for a photon to break apart a Cooper pair, making it accessible experimentally at low temperatures.

Deeper insight into the mechanism leading to a finite electric dipole for the phase modes is then gained through a comparison with the XY model in transverse random field. Within this effective *bosonic* description of disordered superconductors [31,32] the randomness of the transverse field induces an inhomogeneity of the local superfluid stiffness quite different from the one of uniformly disordered XY

models [12,13]. Indeed, in full analogy with the outcomes of the fermionic Hubbard model [25,26,29,30], the local superfluid stiffness forms, at strong disorder, good SC regions of tens of nanometers embedded in a poorly SC background. Since the dc superfluid current flows along preferential percolative paths through the good SC regions [30], the finite-frequency optical absorption occurs in the remaining isolated SC regions, thanks to the presence of a finite phase difference between the opposite sides of the islands, which then act as nanoantennas. This nanoscale selective optical effect, which we propose to test via microscopic imaging [33], can be used to tune the resonant frequency and the quality factor of superconducting microresonators [34].

II. FERMIONIC MODEL

The model Hamiltonian we consider to investigate a disordered superconductor is the attractive Hubbard model ($U < 0$) with local disorder $V_i \in [-V, V]$ and hopping t restricted to nearest neighbors,

$$H = -t \sum_{\langle ij\rangle\sigma} (c^\dagger_{i\sigma} c_{j\sigma} + \text{H.c.}) + U \sum_i n_{i\uparrow} n_{i\downarrow} + \sum_{i\sigma} V_i n_{i\sigma}, \quad (1)$$

which we solve in the mean field on an $N \equiv N_x \times N_y$ lattice (up to $N = 20 \times 20$ with periodic boundary conditions) by using the Bogoliubov–de Gennes (BdG) approach [35,36]. The total current in direction α is defined as usual as

$$J_\alpha(\mathbf{q},\omega) = -e^2 K_{\alpha\beta}(\mathbf{q},\omega) A_\beta(\mathbf{q},\omega), \quad (2)$$

$$K_{\alpha\beta}(\mathbf{q},\omega) = D\delta_{\alpha\beta} - \chi_{\alpha\beta}(\mathbf{q},\omega)\,. \quad (3)$$

Here $D = \frac{t}{N} \sum_{n,\sigma} \langle (c^\dagger_{n,\sigma} c_{n+\hat{\alpha}\sigma} + \text{H.c.}) \rangle$ is the diamagnetic term, where $\langle \cdots \rangle$ denotes the thermal and disorder average, which restores the translational invariance for model (1), allowing one to define the Fourier transform $\chi_{\alpha\beta}(\mathbf{q},\omega)$ of the correlation function for the paramagnetic current $j^\alpha_n = -it \sum_\sigma [c^\dagger_{n\sigma} c_{n+\hat{\alpha},\sigma} - c^\dagger_{n+\hat{\alpha},\sigma} c_{n\sigma}]$. In a superconductor the superfluid stiffness is defined by the transverse $\mathbf{q} \to 0$ limit of Eq. (2). For example, for a field along the x direction one has $J_x = -e^2 D_s A_x$, where

$$D_s = D - \text{Re}\,\chi_{xx}(q_x = 0, q_y \to 0, \omega = 0). \quad (4)$$

The optical conductivity is obtained from Eq. (2) by assuming a homogeneous vector potential, so that

$$A_x(\omega) = \frac{E_x(\omega)}{i\omega}, \quad (5)$$

and the real part of the optical conductivity is

$$\sigma(\omega) = -e^2 \text{Re}\, \frac{K_{xx}(\mathbf{q} = 0, \omega)}{i(\omega + i0^+)}, \quad (6)$$

leading to

$$\sigma(\omega) = e^2 \pi \delta(\omega)[D - \text{Re}\,\chi_{xx}(\mathbf{0},\omega)] + e^2 \frac{\text{Im}\,\chi_{xx}(\mathbf{0},\omega)}{\omega}$$
$$\equiv e^2 \pi D_s \delta(\omega) + \sigma_{\text{reg}}(\omega), \quad (7)$$

where we separated explicitly the superfluid response at $\omega = 0$ from the regular part σ_{reg} occurring at finite frequency. By

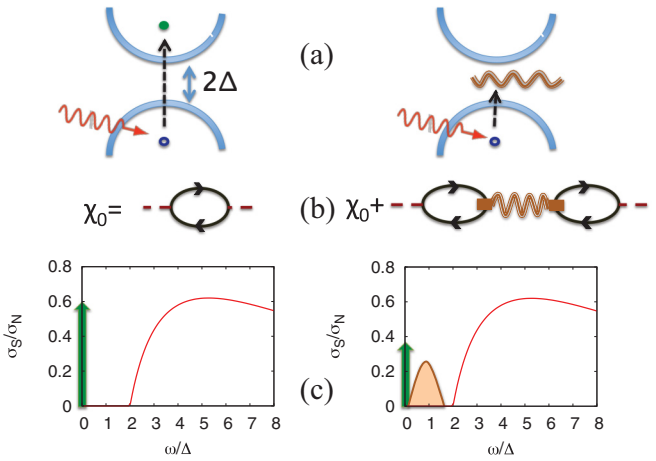

FIG. 1. (Color online) Schematic of the optical absorption σ_S/σ_N (S = SC, N = normal state) in a disordered superconductor. (left) In the BCS approach only (a) the single-particle excitations across the SC gap 2Δ are included, corresponding to the (b) bare-bubble approximation for the current-current response function. (c) The resulting optical conductivity consists of a Δ peak at $\omega = 0$ of weight D_s^{BCS} (arrow) plus a regular part (solid line) starting at $\omega = 2\Delta$. (right) When vertex corrections are included, (a) an excited quasiparticle can be converted in a collective mode, described in (b) the diagrammatic approach by the RPA resummations of the corresponding amplitude, phase, or density fluctuations. (c) An additional absorption appears at energies $\omega < 2\Delta$, corresponding to a superfluid peak at $\omega = 0$ with strength $D_s < D_s^{BCS}$.

using the Kramers-Kronig relations for χ_{xx} one then finds the well-known optical sum rule

$$\int_0^\infty d\omega \sigma(\omega) = \frac{\pi e^2}{2} D_s + \int_{0^+}^\infty \sigma_{\text{reg}}(\omega) = \frac{\pi e^2}{2} D. \quad (8)$$

Equation (8) shows that any paramagnetic process described by σ_{reg} leads to a suppression of the superfluid stiffness with respect to the diamagnetic term D, which at small density and weak interactions reduces to the usual form $D \simeq n/m$. In the BCS theory $\chi \equiv \chi_0$ is computed in the so-called bare-bubble approximation [see Fig. 1(b), left] [35], in which one includes only particle-hole excitations on top of the BCS ground state. At $T = 0$ these excitations are exponentially suppressed by the opening of the gap, so that the optical absorption is possible only above the threshold to break a Cooper pair, i.e., at $\omega > \omega_{\text{pair}} = 2\Delta$ [see Fig. 1(c), left]. Provided that ω_{pair} is smaller than the inverse lifetime of quasiparticles, the resulting $\sigma_{\text{reg}}^{BCS}(\omega)$ is given by the well-known Mattis-Bardeen formula [37], and the superfluid stiffness D_s^{BCS} is smaller than D already at $T = 0$. In the following we will also show that collective modes, neglected in the BCS approach, give rise to a finite contribution to $\sigma_{\text{reg}}(\omega)$ at strong disorder, which is located mainly below ω_{pair} [see Fig. 1(c), right]. This additional optical absorption is accompanied by a further reduction of D_s with respect to D_s^{BCS} [30], which has been experimentally reported [4,15,16].

The full optical response beyond the BCS level can be computed by including vertex corrections [35], which also guarantee full gauge invariance of the theory [35,38]. The

current-current correlation function χ can then be expressed in a compact form as (see Appendix A)

$$\chi = \chi_0 + \hat{\Lambda}^T V[1 - \hat{\Pi}^0 V]^{-1}\hat{\Lambda}, \tag{9}$$

where $\hat{\Lambda}$ is the vector containing the correlation functions that couple the current j_n^α to collective modes, i.e., particle-particle (amplitude and phase) and density fluctuations, described by the random-phase approximation (RPA) resummation of the bare susceptibility $\hat{\Pi}^0$ [see Fig. 1(b), right]. $\hat{V}$ and $\hat{\Pi}^0$ are matrices both in real space and in the phase space of collective modes, and translational invariance for χ is recovered after averaging over disorder configurations. In the clean case collective modes contribute only to the longitudinal response at finite $\mathbf{q}$ [35,38]. In contrast, disorder renders the $\hat{\Lambda}$ susceptibilities finite even for a $\mathbf{q} = 0$ external perturbation, so that the collective modes contribute to the optical response. Notice that this optical mechanism is similar to the one discussed recently for few-layer graphene [39] to explain the huge infrared-phonon peaks [40]. In that case doping activates the intermediate particle-hole process, analogous to what disorder does in our problem.

The results for the optical conductivity at finite frequency for two representative values of coupling U and disorder are shown in Fig. 2, along with their BCS counterparts. As one can see, the major differences between the two appear below the scale $\omega_{\rm pair} = 2\Delta$, marked with a dashed line. Notice that in the model (1) the spectral gap Δ in the single-particle excitations remains finite (and relatively large) at strong disorder, as has been discussed previously [25,26,29]. As a consequence, the BCS calculation always shows a finite threshold at $\omega_{\rm pair}$, with a profile that coincides at low disorder with the Mattis-Bardeen prediction [37]. In contrast, the full response extends also below $\omega_{\rm pair}$, with a shape and intensity that depend on both the SC coupling U and disorder. This result

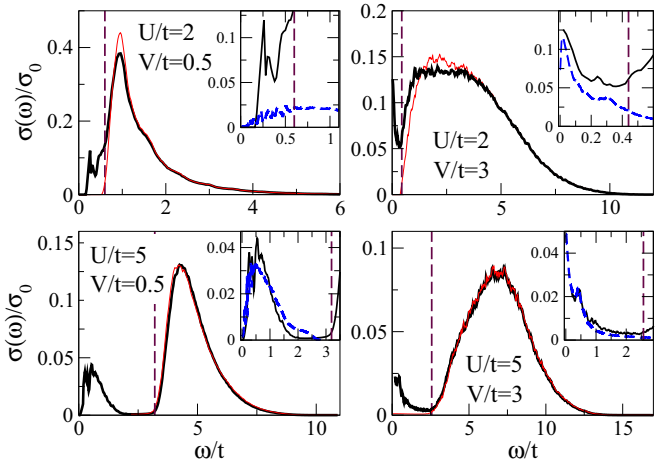

FIG. 2. (Color online) $\sigma(\omega)$ in units of $\sigma_0 \equiv e^2/\hbar$ for the fermionic model (1). Here $N = 20 \times 20$ and we averaged over 50 disorder configurations. The main panels report the curves without (thin red line) and with (thick black line) vertex corrections, while the dashed vertical lines mark $\omega_{\rm pair} = 2\Delta$. The insets show a zoom of the low-energy part along with the results of the bosonic model (10) (dashed lines), with W and J parameters assigned as described in the text.

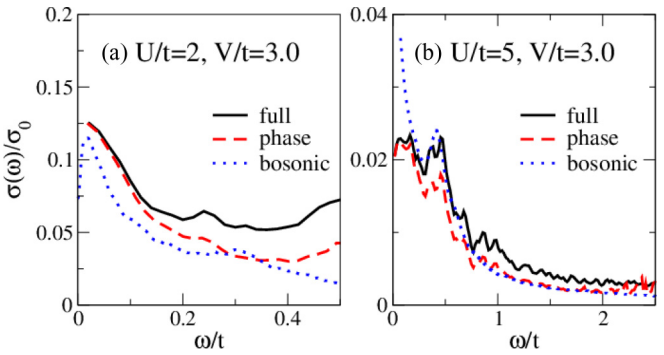

FIG. 3. (Color online) Comparison between $\sigma(\omega)$ computed using the full gauge-invariant response (solid black line) and the contribution of phase fluctuations only (dashed red line; see Appendix A). The results of Fig. 2 for the bosonic model (10) (dotted blue line) are reported as well.

can explain the residual optical absorption in the microwave regime [14,17] and deviations from BCS theory [4,15,16] observed recently at strong disorder. In particular, the smearing of the $\omega_{\rm pair}$ threshold due to the presence of a dissipative channel associated with phase modes can lead to an apparent optical gap smaller than the one measured by STM, explaining the puzzling results of Ref. [17]. At the same time this effect can influence the performance of superconducting microwave devices, a field that has grown dramatically over the past decade [34]. Finally, two remarks are in order with respect to the results of Fig. 2. First of all, we checked that even though all the collective modes enter in the full response, the main contribution to $\sigma_{\rm reg}(\omega)$ at low energy stems from phase fluctuations. This is shown explicitly in Fig. 3, where $\sigma_{\rm reg}(\omega)$ has been computed by including only the phase-current vertex in Eq. (9) (see Appendix A). Second, one could wonder what happens when the Coulomb interaction, neglected in the present calculations, is taken into account. Indeed, it is well known that in the presence of long-range interactions the soundlike dispersion of phase modes is converted into a plasmonic one [38]. However, while this effect appears dramatically in the dielectric function, it tends to cancel out in the optical conductivity, as discussed in Appendix C. While in the clean case the cancellation is exact, leaving only soundlike modes in the optical conductivity, for weak disorder it is still a good approximation, as discussed in Ref. [41]. For strong disorder the mixing between the transverse and longitudinal responses could move part of the optical spectral weight to the plasma energy, but its explicit investigation is beyond the scope of the present paper.

III. BOSONIC MODEL

To systematically address the structure of the phase excitations responsible for the subgap absorption we also compute the optical conductivity within an effective bosonic model for the disordered superconductor, i.e., the XY spin-1/2 model in a transverse random field [31]:

$$\mathcal{H}_{PS} \equiv -2\sum_i \xi_i S_i^z - 2J\sum_{\langle i,j\rangle}(S_i^+ S_j^- + \text{H.c.}). \tag{10}$$

In the pseudospin language $S^z = \pm 1/2$ corresponds to a site occupied or unoccupied by a Cooper pair, while superconductivity corresponds to a spontaneous in-plane magnetization, e.g., $\langle S_i^x \rangle \neq 0$. Disorder is represented by the random transverse field ξ_i, box distributed between $-W$ and W. The optical response of classical [12] and quantum [13] XY-like models has been addressed previously by introducing disorder in the coupling J. The model (10) focuses instead on the competition between pair hopping J and localization W [31,42–44], which has recently been proven to describe successfully [5,43] the STM experimental results in the SC phase near the SIT. We first solve the model (10) in the mean field to determine $\langle S_i^x \rangle = \frac{1}{2} \sin\theta_i$ and then rotate to the local coordinate system such that the new z axis is $\widetilde{S}_i^z = S_i^z \cos\theta_i + S_i^x \sin\theta_i$. At strong disorder the SC order parameter develops an inhomogeneous spatial distribution, with SC islands embedded in an insulating background (see Fig. 6 below), in analogy both with the fermionic model (1) [25,26,30] and with tunneling experiments [5,8]. Small fluctuations with respect to the mean-field configuration can be described by means of a Holstein-Primakov (HP) scheme, where spins are bosonized as usual as $\widetilde{S}_i^z = 1/2 - a_i^+ a_i$, $\widetilde{S}_i^+ \simeq a_i$, and $\widetilde{S}_i^- \simeq a_i^+$. Here we have defined $\widetilde{S}_i^{\pm} = \widetilde{S}_i^x \pm i\widetilde{S}_i^y$, with $\widetilde{S}_i^x = -S_i^z \sin\theta_i + S_i^x \cos\theta_i$ and $\widetilde{S}_i^y = S_i^y$ being orthogonal to the local quantization axis. The Hamiltonian (10) is then mapped into a quadratic model $\mathcal{H}_{PS} = E_{MF} + \mathcal{H}'_{PS}$ that can be diagonalized by means of a Bogoliubov transformation $a_i = \sum_\alpha (u_{\alpha i}\gamma_\alpha + v_{\alpha i}\gamma_\alpha^\dagger)$:

$$\mathcal{H}'_{PS} = \sum_{ij}\left[A_{ij}(a_i^\dagger a_j + \text{H.c.}) + \frac{1}{2}B_{ij}(a_i a_j + \text{H.c.})\right] = \sum_\alpha E_\alpha \gamma_\alpha^\dagger \gamma_\alpha + \text{const.} \quad (11)$$

Here $A_{ij} = 2\delta_{ij}\xi_i/\cos\theta_i - J(1+\cos\theta_i\cos\theta_j)(1-\delta_{ij})$ and $B_{ij} = J(1-\cos\theta_i\cos\theta_j)(1-\delta_{ij})$ are the matrices that enter in the eigenvalue problem for the excitation energies E_α [45]. The equivalence between the HP excitations and the SC phase excitations at the Gaussian level can be made explicit by the identification of the phase operators Φ_i and their conjugated momenta L_i,

$$\Phi_i = -2\frac{S_i^y}{\sin\theta_i} = \sum_\alpha i\frac{\phi_{\alpha i}}{\sqrt{2}}(\gamma_\alpha^\dagger - \gamma_\alpha), \quad (12)$$

$$L_i = S_i^\perp \sin\theta_i = \sum_\alpha \frac{\ell_{\alpha i}}{\sqrt{2}}(\gamma_\alpha^\dagger + \gamma_\alpha), \quad (13)$$

where $\phi_{\alpha i} = \sqrt{2}(v_{\alpha i} - u_{\alpha i})/\sin\theta_i$ and $\ell_{\alpha i} = (u_{\alpha i} + v_{\alpha i})\sin\theta_i/\sqrt{2}$. The fluctuation part of the Hamiltonian (11) can then be expressed as

$$\mathcal{H}'_{PS} = \frac{1}{2}\sum_{i,\mu=x,y} J_i^\mu [\Delta_\mu \Phi_i]^2 + \frac{1}{2}\sum_{ij}\mathcal{X}_{ij}^{-1} L_i L_j, \quad (14)$$

where $J_i^\mu \equiv J\sin\theta_i \sin\theta_{i+\hat{\mu}}$ are the local stiffnesses of the disordered superconductor, Δ_μ is the discrete derivative in the μ direction, and $\mathcal{X}_{ij}^{-1} = 2(A_{ij} + B_{ij})/\sin\theta_i \sin\theta_j$ is the inverse matrix of the compressibilities. Consistent with the identification (12) the usual Peierls coupling to the gauge field in the pseudospin model (10) corresponds to the replacement $S_i^+ S_{i+\mu}^- \to S_i^+ S_{i+\mu}^- e^{-2ieA_\mu}$, with a factor of 2 accounting for the double charge of each Cooper pair. This leads in Eq. (14) to the shift $\Delta_\mu \Phi_i \to \Delta_\mu \Phi_i - 2eA_\mu$, i.e., the usual minimal-coupling scheme. The real part of the optical conductivity for the bosonic model (10) is then easily obtained as $\sigma^B(\omega) = e^2\pi\delta(\omega)D_s^B + \sigma_{\text{reg}}^B(\omega)$, with

$$D_s^B = D^B - \frac{1}{N}\sum_\alpha Z_\alpha, \quad (15)$$

$$\sigma_{\text{reg}}^B(\omega) = \frac{e^2\pi}{2N}\sum_\alpha Z_\alpha[\delta(\omega + E_\alpha) + \delta(\omega - E_\alpha)], \quad (16)$$

where $D^B = (1/N)\sum_i 4J_i^\mu$ is the diamagnetic term of the bosonic model (10), $\mu = x$, for instance, and the effective dipole Z_α of each excitation mode is

$$Z_\alpha = \frac{1}{E_\alpha}\left[\sum_i 2J_i^\mu \Delta_\mu \phi_{\alpha i}\right]^2. \quad (17)$$

For a uniform stiffness (J_i^μ =const) one finds that Z_α is proportional to the total derivative of the phase modulation, which then vanishes for periodic boundary conditions. Thus, the inhomogeneity of J_i^μ induced by disorder is a crucial prerequisite to obtain a finite electric dipole, which is responsible for $\sigma_{\text{reg}}(\omega)$ shown in Fig. 4. As one can see, the optical response moves towards decreasing energies for increasing disorder (i.e., W/J), and its total spectral weight $\int_{0^+}^\infty d\omega\sigma_{\text{reg}}(\omega) = (\pi/2)(D^B - D_s^B)$ [see Eqs. (15) and (16)] first increases, due to the disorder-tuned optical absorption at finite ω, and then decreases again, due to the strong suppression by disorder of the diamagnetic term D^B itself (see the inset in Fig. 4). Notice that the decrease of D^B with increasing disorder reflects the suppression of the local order parameter, encoded in the fermionic language (1) in the suppression of the BCS stiffness D_s^{BCS}. This analogy can be used to obtain a quantitative comparison between the fermionic and the bosonic approaches by fixing W/J of the model (10) in order to reproduce $D_s^B/D^B = D_s/D_s^{BCS}$. In this way we can account in both models for the same transfer of spectral weight from $\omega = 0$ to

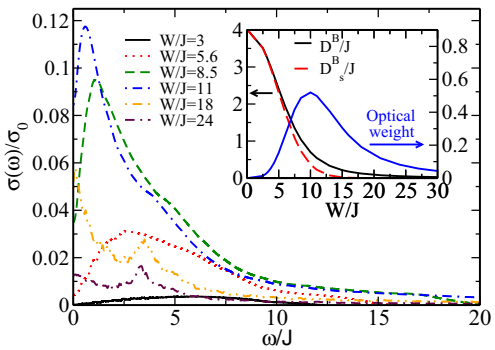

FIG. 4. (Color online) $\sigma_{\text{reg}}(\omega)/\sigma_0$ for the bosonic model (10) at different values of W/J. The lattice size is $N = 50 \times 50$, and the average is taken over 100 disorder configurations. The inset shows the disorder dependence of the diamagnetic term D^B, the superfluid stiffness D_s^B, and the total spectral weight $\int_{0^+}^\infty d\omega\sigma_{\text{reg}}(\omega) = (\pi/2)(D^B - D_s^B)$ in units of J.

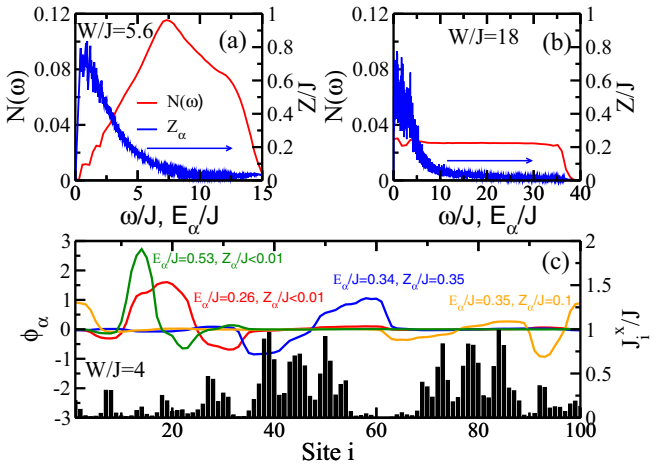

FIG. 5. (Color online) (a) and (b) Density of phase modes $N(\omega)$ and effective dipole Z_α at two values of disorder (averaged over 100 disorder configurations). (c) Spatial structure of the phase modes $\phi_{\alpha i}$ in the one-dimensional case for a given disorder realization. The solid lines represent the spatial dependence of the eigenfunctions $\phi_{\alpha i}$ [whose gradient enters Eq. (17) for the effective dipole Z_α] at selected values of the excitation energies E_α. In the lower part of the figure we also represent with bars the spatial variations of the local stiffness J_i^x. As one can see, the largest effective dipole Z_α is realized for the blue and orange excitations, whose monotonic phase variations overlap with a region of large local stiffness.

$\sigma_{\rm reg}(\omega)$ (see Appendix B). The results are shown in Fig. 3 and in the inset of Fig. 2. As one can see, at large U the bosonic model reproduces in a quantitative way the characteristic energy scales for optical absorption in the fermionic model. At weaker coupling the comparison is instead only qualitative, due partly to the difficulties of clearly separating the contribution of quasiparticles and collective modes.

Let us finally analyze the connection between the optical response and the inhomogeneous spatial distribution of the SC properties. The optical response (16) is proportional to the density of states of phase modes $N(\omega)$, weighted by the effective dipole function Z_α of Eq. (17). Both quantities depend on disorder, as shown in Figs. 5(a) and 5(b), and in general the $1/E_\alpha$ prefactor of Eq. (17) favors a larger dipole for lower-energy modes. In addition at strong disorder, when the system segregates into SC islands with large local stiffness J_μ^i, the optical absorption is large when the phase excitations occur *inside* the SC regions, according to Eq. (17). This effect can be better visualized in a one-dimensional version of the model (10), as shown in Fig. 5(c). Here one can clearly see that the largest optical dipole is realized when a monotonic phase variation overlaps with a good SC region. Since the charge is the conjugate variable of the phase gradients, one then realizes a charge unbalance on the two sides of the island, making it optically active.

At strong disorder this space-selective optical absorption is strictly connected to the emergence of percolative paths for the superfluid currents, analogous to the ones discussed in Ref. [30] for the fermionic model (1). In Fig. 6 we show at two values of W/J the currents in the presence of a finite applied field $\mathbf{A} = -A\hat{x}$ for a given disorder configuration, superimposed on the map of the local stiffnesses J_i^x. Since

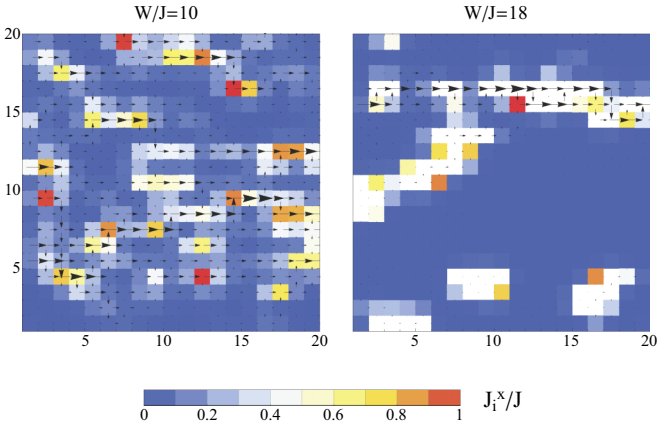

FIG. 6. (Color online) Local supercurrents (arrows) for an applied field $\mathbf{A} = -A\hat{x}$ superimposed over the map of the local stiffnesses J_i^x/J for a given disorder realization and two values of W/J. The size of the arrows is proportional to the strength of the total local current, whose diamagnetic contribution is proportional to the local stiffness displayed in the underlying map. The current flows along preferential paths connecting the regions with large J_i^x. This means that the isolated SC islands, i.e., those which reside far from the main percolative paths of the current, have a large paramagnetic response responsible for the absorption at finite frequencies. For example, for $W/J = 18$ the whole diamagnetic contribution of the white regions on the bottom of the map is transferred to $\sigma_{\rm reg}(\omega)$.

J_i^x is a measure of the local diamagnetic response, a small current occurring over a good SC region is due to a large local paramagnetic response, i.e., to an optical absorption at finite frequencies. At strong disorder the percolative supercurrent paths leave aside several isolated SC islands, which then contribute to $\sigma_{\rm reg}(\omega)$ thanks to the dipole-activation mechanism explained above.

IV. CONCLUSIONS

In summary, we computed the optical response due to collective modes in two prototype fermionic and bosonic models for disordered superconductors. In both cases we find that disorder renders phase fluctuations optically active, in a range of energies that lies below the threshold for single-particle excitations for the fermionic case. The bosonic approach allows us to establish a clear correspondence between the optical response and the spatial inhomogeneity of the SC order parameter, showing that optical absorption stems predominantly from phase fluctuations within the good SC regions. Besides explaining recent experiments in strongly disordered superconductors [14–17] our results could be further checked experimentally by means of near-field scanning microwave impedance microscopy [33]. Indeed, the proposed mechanism of direct correspondence between the SC granularity and optical absorption, evidenced in Fig. 6, can be potentially mapped out by this technique, which is able to resolve spatial variations at length scales well below the radiation wavelength. In this respect the variation of the microwave optical properties of disordered superconductors at the nanoscale can be used to improve the performance of SC microresonators built in standard geometries or even to design new nanoelectric devices targeted for space- and frequency-selective applications.

ACKNOWLEDGMENTS

We thank E. Driessen, A. Frydman, and D. Sherman for useful discussions. L.B. acknowledges financial support by MIUR under Grant No. FIRB2012 (RBFR1236VV).

APPENDIX A: OPTICAL CONDUCTIVITY FOR THE FERMIONIC MODEL

In order to compute fluctuations on top of the inhomogeneous BdG ground state we evaluate dynamical correlation functions

$$\chi_{nm}(\hat{X},\hat{Y}) = -i\int dt e^{i\omega t}\langle \mathcal{T}\hat{X}_n(t)\hat{Y}_m(0)\rangle, \tag{A1}$$

where $\hat{X},\hat{Y}$ correspond to either pair or charge fluctuation operators, i.e., $\delta\Delta_i \equiv c_{i\downarrow}c_{i\uparrow} - \langle c_{i\downarrow}c_{i\uparrow}\rangle_0$, $\delta\Delta_i^\dagger \equiv c_{i\uparrow}^\dagger c_{i\downarrow}^\dagger - \langle c_{i\uparrow}^\dagger c_{i\downarrow}^\dagger\rangle_0$, and $\delta n_i \equiv \sum_\sigma (c_{i\sigma}^\dagger c_{i\sigma} - \langle c_{i\sigma}^\dagger c_{i\sigma}\rangle_0)$. Here and in the following a naught subscript or superscript denotes evaluation in the BdG ground state.

The local interactions between pair ($U\delta\Delta_i^\dagger\delta\Delta_i$, $U\delta\Delta_i\delta\Delta_i^\dagger$) and charge ($U/2\delta n_i\delta n_i$) fluctuations are contained in the matrix $\underline{\underline{V}}$ so that the resummation

$$\underline{\underline{\chi}} = [\underline{\underline{1}} - \underline{\underline{\chi^0}}\,\underline{\underline{V}}]^{-1}\underline{\underline{\chi^0}} \tag{A2}$$

allows us to compute the dynamical amplitude $A_i \equiv (\delta\Delta_i + \delta\Delta_i^\dagger)/\sqrt{2}$ and phase $\Phi_i \equiv (\delta\Delta_i - \delta\Delta_i^\dagger)/\sqrt{2}$ correlations.

Vertex corrections to the bare current-current correlation function $\chi^0_{nm}(j^\alpha,j^\beta)$ can be obtained by defining $\Lambda^\alpha_{nm} = \chi^0_{nm}(j^\alpha,\hat{Y})$ and $\overline{\Lambda}^\alpha_{mn} = \chi^0_{mn}(\hat{Y},j^\alpha)$, which couple the current j^α_n between sites R_n and $R_{n+\hat{\alpha}}$ to the pair and charge fluctuations $\hat{Y}_m \equiv (A_m,\Phi_m,\delta n_m)$. The full (gauge-invariant) current correlation function is then obtained from

$$\begin{aligned}\chi_{nm}\left(j^\alpha_n,j^\beta_m\right) &= \chi^0_{nm}\left(j^\alpha_n,j^\beta_m\right) + \Lambda^\alpha_{nm}V_{mk}\overline{\Lambda}^\beta_{km}\\ &\quad + \Lambda^\alpha_{nm}V_{mk}\chi_{kl}V_{ls}\overline{\Lambda}^\beta_{sm}\\ &= \chi^0_{nm}\left(j^\alpha_n,j^\beta_m\right) + \Lambda^\alpha_{nm}V_{mk}[\underline{\underline{1}} - \underline{\underline{\chi^0}}\,\underline{\underline{V}}]^{-1}_{kl}\overline{\Lambda}^\beta_{lm}.\end{aligned} \tag{A3}$$

The average over several disorder configurations (typically 50–70) restores translational invariance for χ_{nm}, so that $\sigma(\omega)$ can be computed according to Eq. (7). The predominant role of phase fluctuations for the subgap optical response is demonstrated in Fig. 3, where the dashed lines correspond to $\sigma(\omega)$ computed by including only the phase-current vertex in Eq. (A3), whereas the solid lines correspond to the full optical conductivity, dressed by all the collective modes.

APPENDIX B: COMPARISON BETWEEN THE BOSONIC AND FERMIONIC MODELS

In order to make a quantitative comparison between the bosonic and fermionic models we propose a scheme based on the equivalence of the optical spectral weight due to collective modes in both models. In the fermionic model the diamagnetic term D is only weakly dependent on disorder. On the other hand, the BCS estimate of the superfluid density D_s^{BCS} is strongly suppressed due to the enhanced paramagnetic contribution of quasiparticles. In the bosonic model quasiparticle excitations are not present; however, the localization effects due to disorder are taken into account in the effective local stiffnesses J_i^μ, which enter in the bosonic diamagnetic term D^B. Any additional correction due to phase fluctuations is encoded in the ratio D_s/D_s^{BCS} or D_s^B/D^B for the fermionic or bosonic model, respectively. The ratio D_s/D_s^{BCS} also measures the relative strength of the subgap optical response with respect to the BCS-like part. However, since this one is also slightly modified by vertex corrections, especially at weak coupling (see red and black lines in Fig. 2), we estimate an effective $\tilde{D}_s^{BCS}$ from the integrated spectral weight at $\omega > 2\Delta$ of the full optical conductivity. Thus, for a given U in the fermionic model (1) we determine W/J in the bosonic model (10) in order to have $D_s^B/D^B = D_s/\tilde{D}_s^{BCS}$. This establishes a rescaling function α such that $W/J = \alpha(V_0/t)$. We then fix a factor γ ($J = \gamma t$) such that $D^B/J = \tilde{D}_s^{BCS}/\gamma t$, and we then plot $\sigma_{\rm reg}$ as a function of ω/t, as shown in the insets of Fig. 2. This procedure reveals that already for $U/t = 5$, i.e., in the intermediate-coupling regime, the ratio J/t obtained in this way is very similar to the value $J/t \sim t/U$ predicted by the exact mapping of the clean attractive Hubbard model onto the pseudospin model [32].

APPENDIX C: OPTICAL CONDUCTIVITY OF THE CLEAN GAUSSIAN PHASE-ONLY MODEL WITH LONG-RANGE INTERACTION

In order to illustrate the effect of the long-range interaction on the optical conductivity we compare the computation of the optical conductivity of the quantum Gaussian phase-only model with and without the effect of the long-range forces in three-dimensional physical space.

As a starting point we take the effective action of a Bose fluid with short-range forces expanded to quadratic order in density and phase fluctuations as appropriate to describe, for example, helium IV [46]. To consider a charged fluid we add the long-range interaction and the coupling with the gauge field. The action reads

$$\begin{aligned}\mathcal{S} = \sum_{\mathbf{q}}\int dt\Bigg\{ &-\delta\rho(\mathbf{q})\frac{\dot{\theta}(-\mathbf{q})}{2e} + \frac{1}{2e^2}\left[\frac{1}{\chi_0} + \lambda v(\mathbf{q})\right]|\delta\rho(\mathbf{q})|^2\\ &+\frac{1}{8}D_s|i\mathbf{q}\theta(\mathbf{q}) + 2e\mathbf{A}(\mathbf{q})|^2\Bigg\}.\end{aligned} \tag{C1}$$

Here D_s is the superfluid stiffness, χ_0 is the "short-range" compressibility, and $v(\mathbf{q}) = 4\pi e^2/q^2$ is the long-range Coulomb interaction. $\lambda = 0$ describes a model with short-range interactions, while $\lambda = 1$ is the model with short- and long-range interactions. We can define "long-range" compressibility by

$$\chi(\mathbf{q}) \equiv \frac{\chi_0}{1 + \lambda v(\mathbf{q})\chi_0}. \tag{C2}$$

Diagrammatically, χ (χ_0) is the reducible (irreducible) compressibility with respect to the Coulomb interaction $v(\mathbf{q})$.

We can use the Euler-Lagrange equation for charge fluctuations to eliminate them in terms of phase fluctuations

$$\delta\rho(\mathbf{q}) = e\chi(\mathbf{q})\frac{\dot{\theta}(\mathbf{q})}{2}.$$

After performing a Wick rotation one obtains the thermodynamic action of the Gaussian phase-only model in Matsubara frequency [38,47,48],

$$S = \frac{1}{8}\sum_{\mathbf{q},\omega_n}\left[\chi(\mathbf{q})\omega_n^2|\theta(\mathbf{q},\omega_n)|^2 + D_s|i\mathbf{q}\theta(\mathbf{q},\omega_n) + 2e\mathbf{A}(\mathbf{q})|^2\right]. \quad \text{(C3)}$$

The electromagnetic kernel is given by

$$e^2 K_{\alpha\beta} = \left.\frac{\partial \ln Z}{\partial A_\alpha(\mathbf{q})\partial A_\beta(-\mathbf{q})}\right|_{\mathbf{A}=\mathbf{0}},$$

with $Z = \int \mathcal{D}\theta e^{-S}$. This leads to Eq. (3) with $D = D_s$ and the current-current response,

$$\chi_{\alpha\beta} = \frac{D_s^2}{4} q_\alpha q_\beta \langle\theta(\mathbf{q},\omega_n)\theta(-\mathbf{q},-\omega_n)\rangle,$$

where the correlator can be computed directly from the action.

We also define a generalized complex conductivity tensor, which is the current response to the time derivative of the vector potential at finite momentum. The generalized conductivity in the real frequency axis reads

$$\bar{\sigma}_{\alpha\beta}(\mathbf{q},\omega) = -e^2\frac{K_{\alpha\beta}(\mathbf{q},\omega+i0^+)}{i(\omega+i0^+)}. \quad \text{(C4)}$$

The relation with the usual conductivity will be discussed below.

We first set $\lambda = 0$ and analyze the short-range model. In this case the current response reads

$$\chi_{\alpha\beta} = -\frac{D_s^2}{\chi_0}\frac{q_\alpha q_\beta}{(i\omega_n)^2 - \omega_{\mathbf{q}}^2},$$

where we defined the sound mode dispersion

$$\omega_{\mathbf{q}}^2 = \frac{D_s q^2}{\chi_0}. \quad \text{(C5)}$$

One can check that the transverse (T) and longitudinal (L) parts do not mix, so we can separate the electromagnetic kernel as

$$K = \frac{q_\alpha q_\beta}{q^2}K_L + \left(\delta_{\alpha\beta} - \frac{q_\alpha q_\beta}{q^2}\right)K_T,$$

with

$$K_L = D_s\frac{(i\omega_n)^2}{(i\omega_n)^2 - \omega_{\mathbf{q}}^2}, \quad K_T = D_s. \quad \text{(C6)}$$

From Eq. (C4) one obtains L and T conductivities,

$$\bar{\sigma}_L^{ir}(\mathbf{q},\omega) = \frac{ie^2 D_s}{2}\left(\frac{1}{\omega+i0^+ + \omega_{\mathbf{q}}} + \frac{1}{\omega+i0^+ - \omega_{\mathbf{q}}}\right),$$
$$\bar{\sigma}_T^{ir}(\mathbf{q},\omega) = \frac{ie^2 D_s}{\omega+i0^+}. \quad \text{(C7)}$$

As expected, in the limit $\mathbf{q}\to 0$ both conductivities coincide, but the longitudinal conductivity, neglecting long-range forces, has a sound pole at finite momentum. Thus, longitudinal fields excite sound modes, as can be expected.

In Eq. (C7) ir stands for "irreducible" with respect to the Coulomb interactions and means that $\bar{\sigma}^{ir}$ is the response to an external field, neglecting the polarization of the medium. As we shall argue below, the polarization of the medium can be taken into account by including its effect on the electric field.

We now repeat the computation in the presence of long-range forces, i.e., setting $\lambda = 1$. Expressions can be obtained from above with the substitution $\chi_0 \to \chi(\mathbf{q})$.

The electromagnetic kernel Eq. (C6) remains the same with the replacement $\omega_{\mathbf{q}} \to \Omega_{\mathbf{q}}$. Thus, one gets the well-known shift of the longitudinal modes to the plasma frequency, $\Omega_0 = 4\pi e^2 D_s$, with a quadratic dispersion for small momentum,

$$\Omega_{\mathbf{q}}^2 = \frac{D_s q^2}{\chi(\mathbf{q})} = \Omega_0^2 + \omega_{\mathbf{q}}^2.$$

Here $\omega_{\mathbf{q}}$ is still given by Eq. (C5). This procedure automatically resums the effect of the long-range interaction in the response function so that the resulting conductivity is a reducible response,

$$\bar{\sigma}_L^{re}(\mathbf{q},\omega) = \frac{ie^2 D_s}{2}\left(\frac{1}{\omega+i0^+ + \Omega_{\mathbf{q}}} + \frac{1}{\omega+i0^+ - \Omega_{\mathbf{q}}}\right),$$
$$\bar{\sigma}_T^{re}(\mathbf{q},\omega) = \frac{ie^2 D_s}{\omega+i0^+}. \quad \text{(C8)}$$

We now reach a paradox since the T and L parts do not fulfill the common expectation that at $\mathbf{q}\to 0$ one should have

$$\bar{\sigma}_L(\mathbf{q}\to 0,\omega) = \bar{\sigma}_T(\mathbf{q}\to 0,\omega). \quad \text{(C9)}$$

To solve this paradox one should examine more carefully the definition of the optical conductivity. The physical conductivity is defined as the response to the electric field $\mathbf{E}$, which is the sum of the displacement field $\mathbf{D}$ and the field due to the polarization of the medium $\mathbf{P}$,

$$\mathbf{E} = \mathbf{D} - 4\pi\mathbf{P}. \quad \text{(C10)}$$

From Maxwell's equation we also have that the longitudinal part of the electric field is related to the sum of the induced charge $\delta\rho$ and the external charges ρ_e,

$$4\pi(\rho_e + \delta\rho) = \nabla\cdot\mathbf{E}, \quad \text{(C11)}$$

$$\mathbf{E} = -\frac{1}{c}\dot{\mathbf{A}} - \nabla\phi. \quad \text{(C12)}$$

We can also separate the potentials into an induced part and an external part,

$$\phi = \phi_{\text{ext}} + \phi_{\text{ind}}, \quad \text{(C13)}$$

$$\mathbf{A} = \mathbf{A}_{\text{ext}} + \mathbf{A}_{\text{ind}}. \quad \text{(C14)}$$

Since the long-range interaction was included in the action, we are working in the Coulomb gauge and $\nabla\cdot\mathbf{A}_{\text{ind}} = 0$. Also without loss of generality we can take $\phi_{\text{ext}} = 0$. It follows that

$$4\pi\delta\rho = -4\pi\nabla\cdot\mathbf{P} = -\nabla^2\phi, \quad \text{(C15)}$$

$$4\pi\rho_e = \nabla\cdot\mathbf{D} = -\frac{1}{c}\nabla\cdot\dot{\mathbf{A}}. \quad \text{(C16)}$$

The last equation shows that the time derivative of the vector potential is related to the longitudinal part of the displacement

D_L. From the definition (C4) we conclude that $\bar{\sigma}_L^{re}$ is the current response to **D**, while the physical conductivity is the response to **E**. We can obtain the physical longitudinal conductivity $\bar{\sigma}_L$ by introducing the longitudinal screening function $D_L = \epsilon_L E_L$. Thus,

$$J_L = \bar{\sigma}_L^{re} D_L = \bar{\sigma}_L E_L,$$

with $\bar{\sigma}_L \equiv \bar{\sigma}_L^{re}\epsilon_L$. Equation (C10) tells us that the effect of the long-range forces has been included in **E**; thus, $\bar{\sigma}_L$ has to be computed as the response to a field neglecting the long-range interaction in the action, i.e., for $\lambda = 0$. We can thus identify the physical conductivity with the irreducible conductivity, $\bar{\sigma}_L = \bar{\sigma}_L^{ir}$, which solves the paradox. Therefore, Eq. (C9) is only valid for the irreducible conductivities. In the transverse case $\sigma_T^{re} = \sigma_T^{ir}$, while in general these responses are different for longitudinal fields.

As a consistency check we can compute the dielectric function. The charged bosons act as polarizable media. The longitudinal current can be defined as the time derivative of the polarization. Assuming a harmonic time dependence,

$$P_L = -\frac{J_L}{i\omega} = -\frac{\bar{\sigma}_L^{ir}}{i\omega} E_L.$$

From the definition of the dielectric function

$$4\pi P_L = (\epsilon_L - 1)E_L$$

one obtains that

$$\epsilon_L = 1 - \frac{4\pi}{i\omega}\bar{\sigma}_L^{ir},$$

in accord with the conclusion that $\bar{\sigma}_L^{ir}$ is the physical conductivity.

From Eq. (C7) one obtains

$$\epsilon_L = \frac{\omega^2 - \Omega_{\mathbf{q}}^2}{\omega^2 - \omega_{\mathbf{q}}^2}, \tag{C17}$$

which correctly has a zero at the frequency of the longitudinal modes, i.e., the plasmons. One can explicitly check that $\bar{\sigma}_L^{ir} = \bar{\sigma}_L^{re}\epsilon$. The transverse conductivity does not get modified by the long-range interaction, and therefore, $\sigma_T = \sigma_T^{irr} = \sigma_T^{red}$ (except for relativistic corrections, which we neglect).

A remarkable conclusion is that the longitudinal conductivity and dielectric function have a pole at the sound modes of the neutral system. Now suppose that we perturb the system, making it inhomogeneous. It is clear that the neutral sound modes will appear as poles of the longitudinal conductivity at zero momentum. For example, if a weak inhomogeneity with characteristic wave vector **Q** is present, one expects that a pole with frequency $\sim\omega_{\mathbf{Q}}$ will appear in the longitudinal conductivity, and by virtue of Eq. (C9), it should also appear in the transverse conductivity. This argument justifies neglecting long-range effects in our computations of the conductivity of the disordered system and explains the presence of structure at the energy of sound modes even if the system is charged.

[1] For a review see, e.g., P. A. Lee, N. Nagaosa, and X.-G. Wen, Rev. Mod. Phys. **78**, 17 (2006).

[2] K. K. Gomes, A. N. Pasupathy, A. Pushp, S. Ono, Y. Ando, and A. Yazdani, Nature (London) **447**, 569 (2007).

[3] B. Sacépé, C. Chapelier, T. I. Baturina, V. M. Vinokur, M. R. Baklanov, and M. Sanquer, Nat. Commun. **1**, 140 (2010).

[4] M. Mondal, A. Kamlapure, M. Chand, G. Saraswat, S. Kumar, J. Jesudasan, L. Benfatto, V. Tripathi, and P. Raychaudhuri, Phys. Rev. Lett. **106**, 047001 (2011).

[5] B. Sacépé, T. Dubouchet, C. Chapelier, M. Sanquer, M. Ovadia, D. Shahar, M. Feigel'man, and L. Ioffe, Nat. Phys. **7**, 239 (2011).

[6] M. Chand, G. Saraswat, A. Kamlapure, M. Mondal, S. Kumar, J. Jesudasan, V. Bagwe, L. Benfatto, V. Tripathi, and P. Raychaudhuri, Phys. Rev. B **85**, 014508 (2012).

[7] Y. Noat, V. Cherkez, C. Brun, T. Cren, C. Carbillet, F. Debontridder, K. Ilin, M. Siegel, A. Semenov, H. W. Hubers, and D. Roditchev, Phys. Rev. B **88**, 014503 (2013).

[8] A. Kamlapure, T. Das, S. Chandra Ganguli, J. B. Parmar, S. Bhattacharyya, and P. Raychaudhuri, Sci. Rep. **3**, 2979 (2013).

[9] C. Richter, H. Boschker, W. Dietsche, E. Fillis-Tsirakis, R. Jany, F. Loder, L. F. Kourkoutis, D. A. Muller, J. R. Kirtley, C. W. Schneider, and J. Mannhart, Nature (London) **502**, 528 (2013).

[10] Actually, the origin of the pseudogap in underdoped cuprate superconductors is still an open problem since it may also involve a second energy scale originating from a competing order (see Ref. [2]).

[11] J. Corson, J. Orenstein, S. Oh, J. O'Donnell, and J. N. Eckstein, Phys. Rev. Lett. **85**, 2569 (2000).

[12] S. Barabash, D. Stroud, and I.-J. Hwang, Phys. Rev. B **61**, R14924 (2000); S. V. Barabash and D. Stroud, *ibid.* **67**, 144506 (2003).

[13] M. Swanson, Y.-L. Loh, M. Randeria, and N. Trivedi, Phys. Rev. X **4**, 021007 (2014).

[14] R. W. Crane, N. P. Armitage, A. Johansson, G. Sambandamurthy, D. Shahar, and G. Grüner, Phys. Rev. B **75**, 094506 (2007).

[15] E. F. C. Driessen, P. C. J. J. Coumou, R. R. Tromp, P. J. de Visser, and T. M. Klapwijk, Phys. Rev. Lett. **109**, 107003 (2012).

[16] P. C. J. J. Coumou, E. F. C. Driessen, J. Bueno, C. Chapelier, and T. M. Klapwijk, Phys. Rev. B **88**, 180505(R) (2013).

[17] D. Sherman, B. Gorshunov, S. Poran, N. Trivedi, E. Farber, M. Dressel, and A. Frydman, Phys. Rev. B **89**, 035149 (2014).

[18] S. Doniach and M. Inui, Phys. Rev. B **41**, 6668 (1990).

[19] K. Damle and S. Sachdev, Phys. Rev. B **56**, 8714 (1997).

[20] D. Podolsky, A. Auerbach, and D. P. Arovas, Phys. Rev. B **84**, 174522 (2011).

[21] I. O. Kulik, O. Entin-Wohlmant, and R. Orbach, J. Low Temp. Phys. **43**, 591 (1981).

[22] C. M. Varma, J. Low Temp. Phys. **126**, 901 (2002).

[23] While the relativistic $O(N)$ model considered in Ref. [20] assumes that amplitude fluctuations have a simple pole at $\omega = m$, in BCS-like superconductors amplitude fluctuations display a square-root singularity $\sim(\omega^2 - m^2)^{-1/2}$ at the mass $m = 2\Delta$ [21, 22].

[24] M. Mondal, A. Kamlapure, S. Chandra Ganguli, J. Jesudasan, V. Bagwe, L. Benfatto, and P. Raychaudhuri, Sci. Rep. **3**, 1357 (2013).

[25] A. Ghosal, M. Randeria, and N. Trivedi, Phys. Rev. B **65**, 014501 (2001).
[26] Y. Dubi, Y. Meir, and Y. Avishai, Nature (London) **449**, 876 (2007).
[27] Y. Dubi, Y. Meir, and Y. Avishai, Phys. Rev. B **78**, 024502 (2008).
[28] A. Erez and Y. Meir, Europhys. Lett. **91**, 47003 (2010).
[29] K. Bouadim, Y. L. Loh, M. Randeria, and N. Trivedi, Nat. Phys. **7**, 884 (2011).
[30] G. Seibold, L. Benfatto, C. Castellani, and J. Lorenzana, Phys. Rev. Lett. **108**, 207004 (2012).
[31] M. Ma and P. A. Lee, Phys. Rev. B **32**, 5658 (1985).
[32] S. Robaszkiewicz, R. Micnas, and K. A. Chao, Phys. Rev. B **23**, 1447 (1981).
[33] K. Lai, H. Peng, W. Kundhikanjana, D. T. Schoen, C. Xie, S. Meister, Y. Cui, M. A. Kelly, and Z.-X. Shen, Nano Lett. **9**, 1265 (2009).
[34] J. Zmuidzinas, Annu. Rev. Condens. Matter Phys. **3**, 169 (2012).
[35] R. S. Schrieffer, *Theory of Superconductivity* (Addison-Wesley, Redwood City, CA, 1964).
[36] P. G. de Gennes, *Superconductivity of Metals and Alloys* (Westview, Boulder, CO, 1966).
[37] D. C. Mattis and J. Bardeen, Phys. Rev. **111**, 412 (1958).
[38] For a discussion of this issue within an effective-action formalism see, e.g., A. Paramekanti, M. Randeria, T. V. Ramakrishnan, and S. S. Mandal, Phys. Rev. B **62**, 6786 (2000); L. Benfatto, A. Toschi, and S. Caprara, *ibid.* **69**, 184510 (2004); H. Guo, C.-C. Chien, and Y. He, J. Low Temp. Phys. **172**, 5 (2013).
[39] E. Cappelluti, L. Benfatto, M. Manzardo, and A. B. Kuzmenko, Phys. Rev. B **86**, 115439 (2012).
[40] A. B. Kuzmenko, L. Benfatto, E. Cappelluti, I. Crassee, D. van der Marel, P. Blake, K. S. Novoselov, and A. K. Geim, Phys. Rev. Lett. **103**, 116804 (2009); Z. Li, C.-H. Lui, E. Cappelluti, L. Benfatto, K.-F. Mak, G. L. Carr, J. Shan, and T. F. Heinz, *ibid.* **108**, 156801 (2012).
[41] D. Belitz, S. De Souza-Machado, T. P. Devereaux, and D. W. Hoard, Phys. Rev. B **39**, 2072 (1989).
[42] L. B. Ioffe and M. Mezard, Phys. Rev. Lett. **105**, 037001 (2010); M. V. Feigel'man, L. B. Ioffe, and M. Mézard, Phys. Rev. B **82**, 184534 (2010).
[43] G. Lemarié, A. Kamlapure, D. Bucheli, L. Benfatto, J. Lorenzana, G. Seibold, S. C. Ganguli, P. Raychaudhuri, and C. Castellani, Phys. Rev. B **87**, 184509 (2013).
[44] J. P. Álvarez Zúniga and N. Laflorencie, Phys. Rev. Lett. **111**, 160403 (2013).
[45] We verified that the first eigenvalue always corresponds to a zero-energy mode, as expected for the $\mathbf{q} = 0$ limit of the Goldstone mode of the U(1) symmetry broken in the SC phase.
[46] D. Pines and P. Nozières, *The Theory of Quantum Liquids: Superfluid Bose Liquids* (Addison-Wesley, Redwood City, CA, 1990).
[47] T. V. Ramakrishnan, Phys. Scr. T **27**, 24 (1989).
[48] S. De Palo, C. Castellani, C. Di Castro, and B. K. Chakraverty, Phys. Rev. B **60**, 564 (1999).